J. Astrophys. Astr. (1991) **12**, 69–87

Mutual Phenomena of Jovian Satellites

R. Vasundhara *Indian Institute of Astrophysics, Bangalore 560034*

Received 1990 September 20; accepted 1990 December 22

Abstract. Results of the observations of mutual eclipses of Galilean satellites observed from the Vainu Bappu Observatory during 1985 are presented. Theoretical models assuming a uniform disc, Lambert's law and Lommel-Seeliger's law describing the scattering characteristics of the surface of the eclipsed satellite were used to fit the observations. Light curves of the 1E2 event on 1985 September 24 and the 3E1 event on 1985 October 24 observed from VBO and published light curves of the 1E2 event on 1985 September 14, the 3E1 event on 1985 September 26 and the 2E1 event on 1985 October 28 (Arlot *et al.* 1989) were fitted with theoretical light curves using Marquardt's algorithm. The best fitting was obtained using Lommel-Seeliger's law to describe the scattering over the surface of Io and Europa. During the fitting, a parameter δx_{shift} which shifts the theoretical light curve along the direction of relative motion of the eclipsed satellite with respect to the shadow centre, on the sky plane (as seen from the Sun) was determined along with the impact parameter. In absence of other sources like prominent surface features or non perfect sky conditions which could lead to asymmetric light curves, δx_{shift} would be a measure of the phase correction (Aksnes, Franklin & Magnusson 1986) with an accuracy as that of the midtime. Heliocentric $\Delta\alpha \cos(\delta)$ and $\Delta\delta$ at mid times derived from fitted impact parameters are reported.

Key words: Jupiter's satellites—mutual phenomena, scattering characteristics—phase corrections

1. Introduction

The transit of Jupiter through the nodes of its equator on its orbit twice during its orbital period of 11.6 yr, provides the opportunity for an edge-on view of its equatorial plane from the inner solar system. Inclination of the orbital planes of the Galilean satellites to the planet's equator is very small, therefore for a few months around the time of nodal crossing, the satellites frequently eclipse or occult each other when any two of them are aligned with the Sun or Earth respectively.

Observations of the mutual events provide means of observing positions of the satellites with an accuracy at least two orders of magnitude better than the photographic or eclipse (behind the planet) observations. The first observations of mutual phenomena were made in 1973 (Aksnes & Franklin 1976; Arlot, Camichel & Link 1974). The mutual phenomena in 1979 (Arlot 1982) and in 1985–86 were observed extensively (Arlot *et al.* 1989; GSO 1990). This paper presents results of observations made at the Vainu Bappu Observatory during 1985.

2. Observations

The observations were made using the 102 cm reflector and a single channel photometer at the Vainu Bappu Observatory (VBO). A narrow band filter in the Hα region (continuum) was used on all occasions except on 1985 October 17. Focal plane diaphragms of diameters 9 or 12 arcsec were used. The red region and small aperture ensured significant reduction in the contribution of the sky background. The recording system consisted of an EMI 9658 phototube and a pulse counting unit with a cyclic buffer, which on keyboard operation, wrapped around to order the last 1048 data points. The integration time for each event was selected based on predicted duration so that the entire event could be captured within the 1048 data points. The sky conditions were generally poor on all days except on 1985 October 24. Table 1(a) lists the log of observations.

3. Data reduction

3.1 *Determination of the Time of Light Minimum*

The time of light minimum of the events was determined by finding the value of n for which the condition

$$\sum_i (y_{n-i} - y_{n+i})^2 = \text{minimum}$$

was satisfied, where the summation was carried out over a span of i points on either side of the trial point n. For each light curve i was selected so as to avoid wings of light curves affected due to the presence of clouds.

Column 2 in Table 1(a) gives the observed times of light minimum T_{mino}. The large uncertainty of ± 25 s for the 1985 November 15 event was due to the broad minimum and poor sky conditions. The observed eclipse depths are given in Table 1(b). The counts were binned at intervals of 5–25 s depending on the signal to noise ratio and then normalized.

The normalized light curve was fitted with a theoretical light curve to derive the impact parameter and information on the scattering characteristics of the surface of the eclipsed satellite.

3.2 *Calculation of the Eclipse Geometry*

The shape of the light curve depends on the sizes of the two satellites, the impact parameter (y), sizes of the umbral and penumbral cones and the relative velocity of the eclipsed satellite (SAT_2) with respect to the eclipsing one (SAT_1) projected on to the plane perpendicular to the shadow axis.

The radii of cross sections of the umbral (R_U) and the penumbral (R_P) cones at the distance of SAT_2 and the projected relative velocity (v) were calculated in the following manner.

Heliocentric equatorial coordinates of Jupiter were calculated from the heliocentric longitude and latitude of the planet published in the Indian Astronomical Ephemeris

Table 1a. Observed and predicted midtimes (UT)

UT Date Event Air mass (1)	Observed times T_{mino} hh:mm:ss (2)	T_{mido} hh:mm:ss (3)	Predicted times T_{midp}(UT) E-2 hh:mm:ss (4)	G-5 hh:mm:ss (5)	*AF** hh:mm:ss (6)	This work hh:mm:ss (7)
85/09/24 1E2 2.8	19:20:37.6 ±2.0 s	19:20:44.2 ±2.0 s	19:20:29	19:20:39	19:20:00	19:20:32
85/10/12 1E2 1.1	13:33:20.2 ±5.0 s	13:33:25.7 ±5.0 s	13:33:12	13:33:17	13:32:42	13:33:11
85/10/17 3E1 1.2	13:23:25.1 ±2.0 s	13:23:29.7 ±2.0 s	13:23:38	13:23:38	13:23:21	13:23:36
85/10/24 3E1 1.7	16:17:14.0 ±2.0 s	16:17:18.9 ±2.0 s	16:17:31	16:17:26	16:17:21	16:17:30
85/11/15 3E1 1.5	14:32:48.2 ±25.0 s	14:30:55.5 ±25.0 s	14:33:25	14:34:01	14:32:33	14:33:21

* Mid umbral time

Table 1b. Observed and predicted eclipse depths

Ut Date Event (1)	Observed eclipse depth % (2)	Obs. (3)	Impact parameter (arcsec) Predicted E-2 (4)	G-5 (5)	This work (6)
85/09/24 1E2	92.2 ±1.6	0.102	0.131	0.151	0.140
85/10/12 1E2	86.25 ±2.4	0.204	0.190	0.171	0.178
85/10/24 3E1	72.15 ±0.8	0.479	0.498	0.501	0.495
85/11/15 3E1	98.82 ±1.0	0.089	0.102	0.097	0.098

(1985) based on the DE-200 ephemeris. The satellite positions were computed using the quick loading routine "KODQIK" along with "EPHEM/E3" and "GALSAT" (Lieske 1980). Correction for light travel time was taken into account by combining the heliocentric equatorial position (X_{s1}, Y_{s1}, Z_{s1}) and velocity ($\dot{X}_{s1}$, $\dot{Y}_{s1}$, $\dot{Z}_{s1}$) of the eclipsing satellite at time T_{s1} when light from the Sun reached it, and the position (X_{s2}, Y_{s2}, Z_{s2}) and velocity ($\dot{X}_{s2}$, $\dot{Y}_{s2}$, $\dot{Z}_{s2}$) of the eclipsed satellite at time T_{s2} when light left it after reflection from its surface towards the observer, reaching him at time T_{obs}. The

heliocentric distances and velocities of the satellites were calculated from

$$R_{sm} = X_{sm} + Y_{sm} + Z_{sm}$$
$$= (X_{Jm} + x_{sm}) + (Y_{Jm} + y_{sm}) + (Z_{Jm} + z_{sm}) \quad (1)$$
$$V_{sm} = \dot{X}_{sm} + \dot{Y}_{sm} + \dot{Z}_{sm}$$
$$= (\dot{X}_{Jm} + \dot{x}_{sm}) + (\dot{Y}_{Jm} + \dot{y}_{sm}) + (\dot{Z}_{Jm} + \dot{z}_{sm}) \quad (2)$$

where (X_{Jm}, Y_{Jm}, Z_{Jm}) and $(\dot{X}_{Jm}, \dot{Y}_{Jm}, \dot{Z}_{Jm})$ are the position and velocity of Jupiter at time T_{sm} $(m=1, 2)$. The positions and velocities of the two satellites along Earth's equatorial coordinates centered at the barycenter of the Jupiter system are (x_{sm}, y_{sm}, z_{sm}) and $(\dot{x}_{sm}, \dot{y}_{sm}, \dot{z}_{sm})$ respectively.

T_{s1} and T_{s2} were obtained iteratively from the observed midtime T_{obs}. The solutions converged within 3 to 4 iterations. The projected relative velocity v and distance d are given by

$$v = V_{s2} \times \sin(\theta_2) \times \cos(\theta_{12}) - V_{s1} \times \sin(\theta_1)$$
$$d = r_{s1s2} \times \sin(u) \quad (3)$$

where θ_{12} is the angle between the two vectors R_{s1} and R_{s2}, θ_m the angle between SAT_m – Sun vector and the direction of motion of the corresponding satellite, and r_{s1s2} is the distance $(x_{s1s2}, y_{s1s2}, z_{s1s2})$ between the two satellites. The angle u between SAT_1 – Sun and $SAT_1 - SAT_2$ vectors is given by:

$$\cos(u) = \left(-\frac{X_{s1}}{R_{s1}}\right) \times \frac{x_{s1s2}}{r_{s1s2}} + \left(-\frac{Y_{s1}}{R_{s1}}\right) \times \frac{y_{s1s2}}{r_{s1s2}} + \left(-\frac{Z_{s1}}{R_{s1}}\right) \times \frac{z_{s1s2}}{r_{s1s2}} \quad (4)$$

The midtimes and impact parameters predicted using this method are given in columns 4–7 of Tables 1(a) and columns 4–6 of 1(b) respectively along with the predictions E-2 and G-5 by Arlot (1984) and AF by Aksnes & Franklin (1984). The impact parameter in column 3 Table 1(b) was calculated from the fitted impact parameter. The radii of cross sections of the umbral and penumbral cones at the distance of the eclipsed satellite were calculated using the following relations (Aksnes 1974):

$$R_u = R_1 \times \frac{R_{s2} - R_{s1} \times \dfrac{R_s}{R_s - R_1}}{R_{s1} - R_{s1} \times \dfrac{R_s}{R_s - R_1}} \quad (5)$$

$$R_p = R_1 \times \frac{R_{s2} - R_{s1} \times \dfrac{R_s}{R_s + R_1}}{R_{s1} - R_{s1} \times \dfrac{R_s}{R_s + R_1}} \quad (6)$$

where R_s and R_1 are the radii of the Sun and the eclipsing satellite respectively. The radii of Io, Europa and Ganymede were taken to be 1815, 1569 and 2631 kms respectively (Morrison 1982)

3.3 *Computation of Light Loss*

The light loss in the umbra and the penumbra were computed using the method described by Aksnes & Franklin (1976) but modified to include the effect of limb darkening on the eclipsed satellite. Fig. 1 shows the geometry for a particular case as seen from the Sun. The eclipsed satellite totally encompasses the umbra UU′ and part of the penumbra (LTIWMKL). Fig. 2 depicts the heliocentric view of SAT_2; S_2 is the centre of the eclipsed satellite, S and E the subsolar and subterrestrial points respectively. The great circle perpendicular to S_2S in the plane ENS_2W is represented as (LTIWMDL) in Fig. 1. The loss in light in the penumbra L_p is given by

$$L_p = \int_{a0}^{a1} l_p(x)x \int_0^{2\pi} \frac{wi \times wt(x)}{p} d\phi dx + \int_{a1}^{a2} l_p(x)x \int_{-\beta}^{+\beta} \frac{wi \times wt(x)}{p} d\phi dx. \qquad (7)$$

The intensity in the penumbra $1-l_p(x)$, at a distance x from the shadow axis was calculated using a method described by Aksnes & Franklin (1976) taking into account the limb darkening on the Sun at the wavelength of observation. $\frac{x\,dx\,d\phi}{p}$ is the elementary area at the point $Q'(\theta, \psi)$ on the surface of SAT_2 of which $x\,dx\,d\phi$ is the projection on the disc at the point Q as seen from the Sun (Fig. 1). If i and e are the

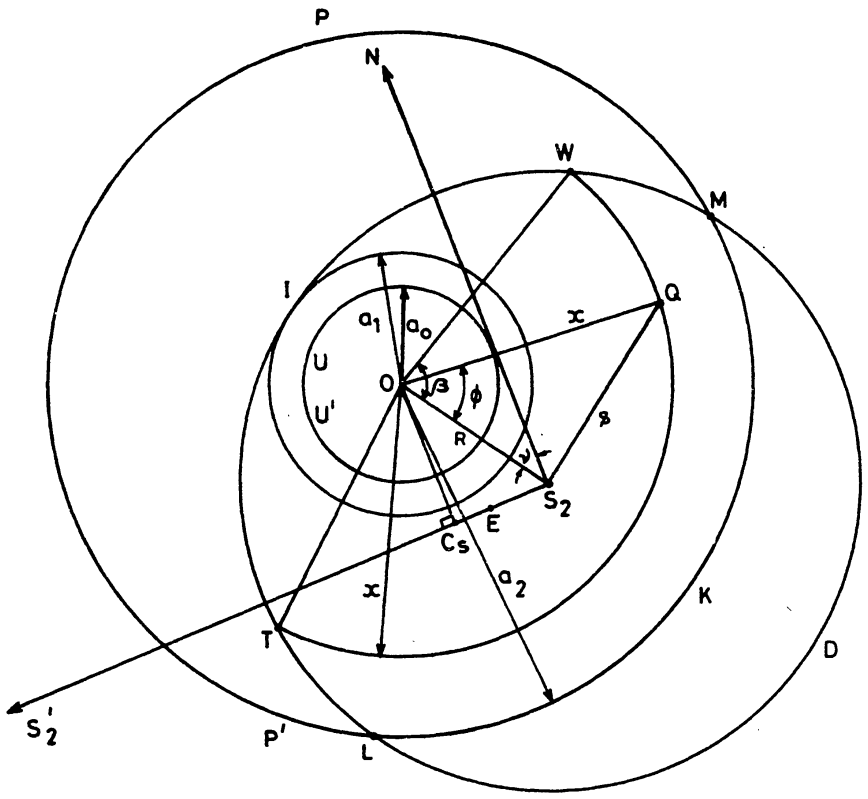

Figure 1. Geometry of eclipse for a particular case when SAT_2 totally encompasses the umbra UU′ and part of the penumbra PP′. O is the shadow centre and S_2 is the centre of SAT_2. Motion of SAT_2 is along $S_2S'_2$.

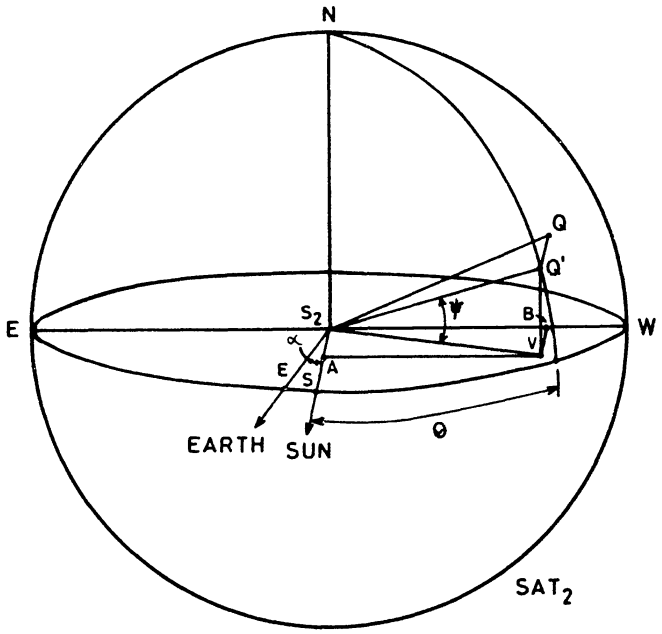

Figure 2. Heliocentric view of SAT_2. $\cos(i)=\mu_0=\cos\psi\cos\theta$, $\cos(e)=\mu_1=\cos\psi\cos(\theta+\alpha)$. The azimuth θ is measured from the subsolar point S in the plane containing centre of SAT_2, S and the subterrestrial point E. S_2N is parallel to Jupiter's spin axis. The point Q' on the surface of SAT_2 is projected as Q on the disc.

angles of incidence and reflectance at the point Q' respectively,

$$\mu_0=\cos(i)$$

$$p=\mu_0$$

$$\mu_1=\cos(e).$$

For the uniform disc model p was set equal to 1. The ratio of intensity at a radial distance s on the disc of SAT_2 to that at its centre is given by

$$wt(x)=\frac{I(s)}{I(0)}$$

$$=\text{constant}\times w. \tag{8}$$

w was calculated assuming a light distribution on the disc of SAT_2 given by

$$w=1 \text{ Uniform disc} \tag{9a}$$

$$=\mu_0\times\mu_1 \text{ Lambert's law (Surdej \& Surdej 1978)} \tag{9b}$$

$$=1-u+u\times\mu \quad \text{with} \quad u=1,\ \mu=\mu_0=\mu_1 \quad \text{and} \quad p=1 \tag{9c}$$

$$=\frac{\mu_0\times\mu_1}{\mu_0+\mu_1} \text{ Lommel-Seeliger's law (Surdej \& Surdej 1978).} \tag{9d}$$

For the point Q' on SAT_2

$$\mu_0=\cos\psi\cos\theta$$

$$\mu_1=\cos\psi\cos(\theta+\alpha). \tag{10}$$

For the eclipse events the longitude is measured more conveniently from S. The plane containing the centres of the Sun, the Earth and the satellites is inclined by less than 0.5 deg. to the orbital planes of the satellites and the equatorial plane of Jupiter, therefore motion of SAT_2 would be very close to this plane; S_2N and C_SO (Fig. 1) would be parallel to the spin axis of Jupiter (Aksnes, Franklin & Magnusson 1986). Fig. 3 shows the terrestrial view of the event; the defect of illumination on SAT_2 would always be either at the leading or the trailing limb, depending on the direction of relative motion between SAT_2 and SAT_1 and the sign of the solar phase angle α. The co-ordinate (θ, ψ) of the point Q' (Fig. 2) can be calculated from the position (x, ϕ) of the corresponding point Q (Fig. 1) using the following relations:

$$\cos\psi\cos\theta = \frac{QQ'}{S_2Q'}$$

$$= \sqrt{1-(S_2Q/R_2)^2}$$

$$= \sqrt{1-(s/R_2)^2}$$

$$\cos\psi\sin\theta = -\frac{S_2B}{R_2}$$

$$= -\frac{S_2Q}{R_2} \times \sin(NS_2Q)$$

$$= -\frac{s}{R_2} \times \sin(OS_2Q - v)$$

$$\sin\psi = \frac{S_2Q}{R_2} \times \cos(NS_2Q)$$

$$= \frac{s}{R_2} \times \cos(OS_2Q - v)$$

$$v = \arctan(d/y) \qquad (11)$$

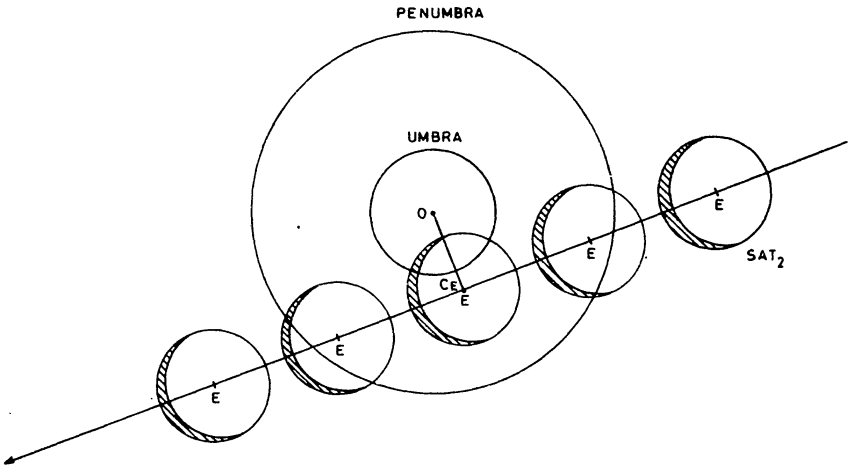

Figure 3. Terrestrial view of the path of SAT_2 across the shadow cone. The defect of illumination on the disc of SAT_2 will be at the leading or trailing limb depending on the direction of its relative motion and the sign of the solar phase angle. C_E is the closest point. OC_E is parallel to Jupiter's spin axis.

where R_2 is the radius of eclipsed satellite, d its distance ($C_S S_2$) from the closest approach point C_S (Fig. 1), and y the impact parameter. Values of μ_0 and μ_1 substituted in Equation 9 yield w in turn to be used in Equation 7. The weight factor wi which takes into account the phase defect on SAT_2 is:

$$wi = 1.0 \text{ for the illuminated regions on } SAT_2$$

$$= 0.0 \text{ for regions beyond the terminator.}$$

The light loss within the umbra is given by

$$L_u = \int_{u0}^{u1} x \int_0^{2\pi} \frac{wi \times wt(x)}{p} d\phi\, dx + \int_{u1}^{u2} x \int_{-\beta}^{+\beta} \frac{wi \times wt(x)}{p} d\phi\, dx \tag{12}$$

where $u0$, $u1$, $u2$, the limits of integration are determined for each instant as in case of the penumbral limits, note that $u0$ is always zero.

The total light loss in the umbra and penumbra was normalized with respect to the total light from the uneclipsed surface of SAT_2, before comparison with the observed data.

The phase correction δx_{phase} suggested by Aksnes, Franklin & Magnusson (1986) as the distance of light centre from the geometric centre, was calculated from the following expression:

$$\delta x_{\text{phase}} = \frac{LM_p + LM_u}{L_p + L_u} \tag{13}$$

where LM_p and LM_u are given by

$$LM_p = \int_{a0}^{a1} l_p(x) x \int_0^{2\pi} \frac{wi \times wt(x)}{p} x \sin(\phi) d\phi\, dx + \int_{a1}^{a2} l_p(x) x \int_{-\beta}^{+\beta} \frac{wi \times wt(x)}{p} x \sin(\phi) d\phi\, dx \tag{14}$$

$$LM_u = \int_{u0}^{u1} x \int_0^{2\pi} \frac{wi \times wt(x)}{p} x \sin(\phi) d\phi dx + \int_{u1}^{u2} x \int_{-\beta}^{+\beta} \frac{wi \times wt(x)}{p} x \sin(\phi) d\phi\, dx. \tag{15}$$

4. The curve fitting and the results

The curve fitting was carried out using Marquardt's algorithm (Bevington 1969). This method searches for the minimum value of χ^2 in an elegant manner by combining the best features of the gradient search method and the method of linearizing the fitting parameters. Such a curve fitting method converges faster than the conventional techniques. The solutions converged to 10^{-9} in $\Delta\chi^2$ within 4 iterations.

The data of the events 1E2 on 1985 September 24 and 3E1 on 1985 October 24 were fitted assuming the laws in Equations 9(a), (b) and (d). Another parameter δx_{shift} was varied simultaneously to shift the theoretical light curve along the direction of motion

Table 2. Results of 1E2 event on 85/09/24. Fitted impact parameters and δx_{shift}.

Model (1)	Limb darkening law (2)	x shift δx_{shift} (kms) (3)	Impact parameter y (kms) (4)	χ^2 (5)	Fig. (6)
Uniform disc	1	(+19)	278	2.224×10^{-4}	4a
Lambert's law	$\mu_0\mu_1$	-58 ± 24	539	0.883×10^{-4}	4b
Lommel-Seeliger's law	$\frac{\mu_0\mu_1}{\mu_0+\mu_1}$	-74 ± 24	328	1.667×10^{-4}	4c

Table 3. Results of 3E1 event on 85/10/24. Fitted impact parameters and δx_{shift}.

Model (1)	Limb darkening law (2)	x shift δx_{shift} (kms) (3)	Impact parameter y (kms) (4)	χ^2 (5)	Fig. (6)
Uniform disc	1	(−25)	1650	0.679×10^{-4}	5a
Lambert's law	$\mu_0\mu_1$	-166 ± 43	1749	1.110×10^{-4}	5b
Lommel-Seeliger's law	$\frac{\mu_0\mu_1}{\mu_0+\mu_1}$	-153 ± 43	1683	0.505×10^{-4}	5c

of SAT_2. The fitted value of δx_{shift} should in principle, be the phase correction. However, asymmetry in the light curve arising due to prominent surface features on SAT_2 or nonperfect sky conditions would have significant contribution to δx_{shift}. Tables 2 and 3 give the fitted values of δx_{shift}, impact parameter and χ^2 for the 2E1 event on 1985 September 24 and 3E1 event of 1985 October 24 respectively, for laws of scattering given in 9(a), (b) and (d). If the motion of SAT_2 relative to SAT_1 is from west to east, a negative value of δx_{shift} indicates that the light centre crossed the close approach point (to shadow centre) before the geometric mid point. Due to contamination of the data due to clouds towards the end of the 1E2 event on 1985 September 24 these points were not used in the fitting. The fitted light curves are shown in Figs 4(a)–(c) and 5(a)–(c) respectively.

The data of 1E2 on 1985 October 12 and 3E1 on 1985 November 11 were also interrupted due to clouds, therefore only portions of the light curves were fitted for y and δx_{shift} assuming the light distribution over SAT_2 to be given by Equation 9(c). A grid search algorithm (Bevington 1969) was employed for fitting these data points. Fitted values of δx_{shift} and impact parameters for these events are given in Table 4; the fitted light curves are shown in Figs 6 and 7 respectively. The fitted theoretical curves are drawn only for the portion that was used in the fitting process. In all the fitted light curves the abscissa is the instantaneous distance ($C_S S_2$ in Fig. 1) of the centre of the eclipsed satellite from the close approach point. This distance can be calculated using

the relation

$$(C_S S_2)_i = \int_{T_{\text{midp}}}^{T_i} v\,dt \tag{16a}$$

or

$$(C_S S_2)_i = (\sqrt{d^2 - y_p^2})_i \tag{16b}$$

where T_{midp} is the predicted time of closest approach and y_p the predicted impact parameter. The distance $C_S S_2$ would be changing at a slightly nonuniform rate

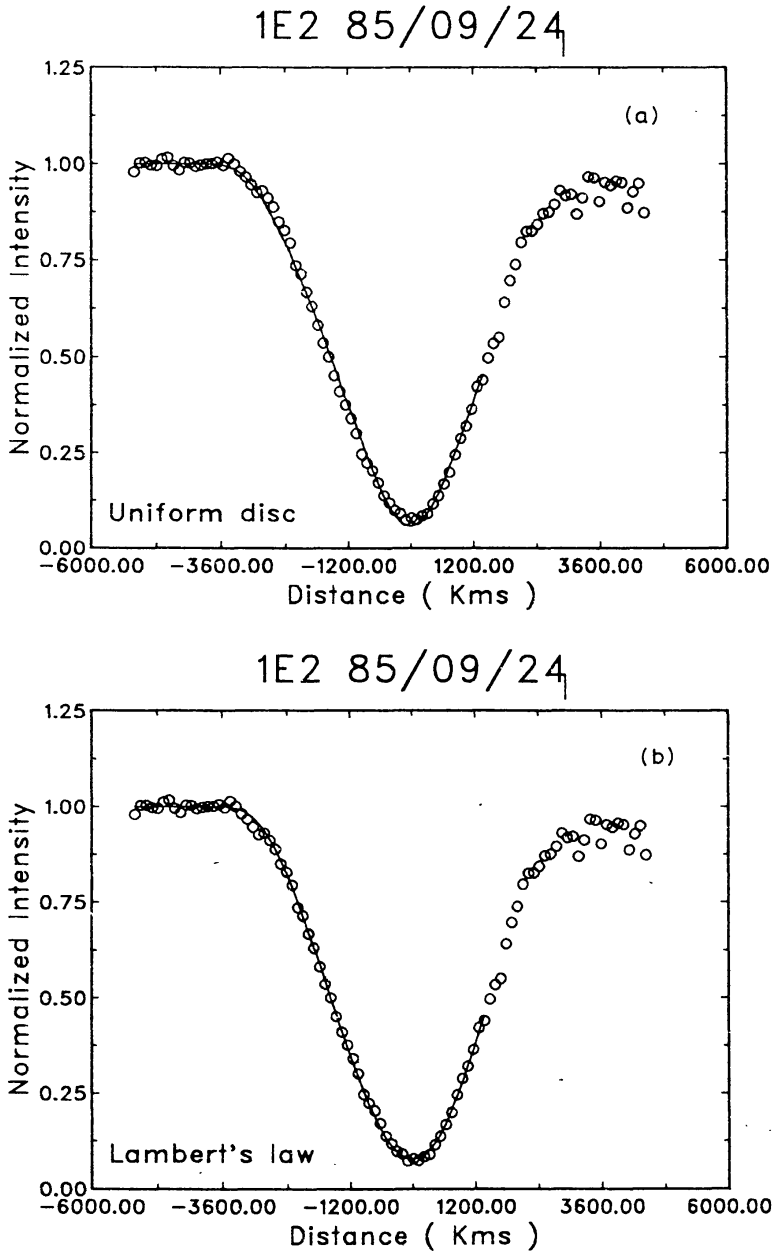

Figure 4. Observed (○) and fitted (continuous line) light curves of 1E2 event on 1985 September 24. The stretch of continuous curve indicates the span of data used in the fitting process; a: uniform disc, b: using Lambert's law, and c: using Lommel-Seeliger's law.

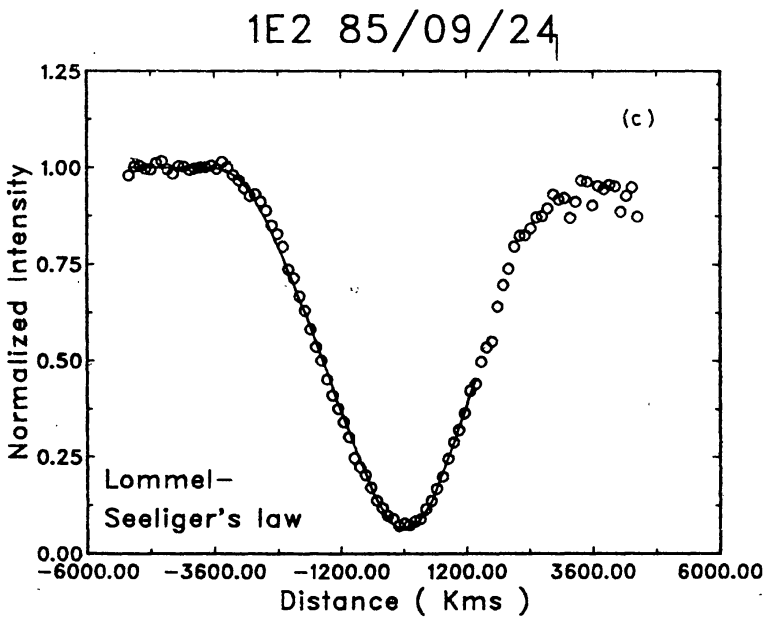

Figure 4. Continued.

because of the variation of v with time. For all the events $C_S S_2$ calculated using 16(a) and 16(b) agreed closely indicating that the motion of SAT_2 relative to the shadow centre can be regarded as linear during the course of the event. The velocity v and acceleration $\dot{v}$ are given in column 3 of Table 6.

Due to uncertainty in the sky measurement for the 3E1 event which occurred during dusk, the data obtained on 1985 October 17 was not analyzed.

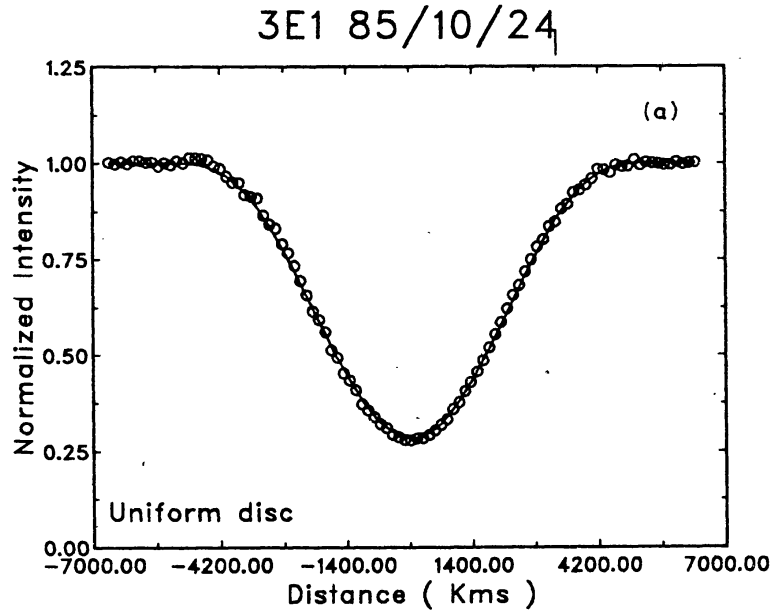

Figure 5. Observed (○) and fitted (continuous line) light curves of 3E1 event on 1985 October 24. Other details same as that given for Fig. 4.

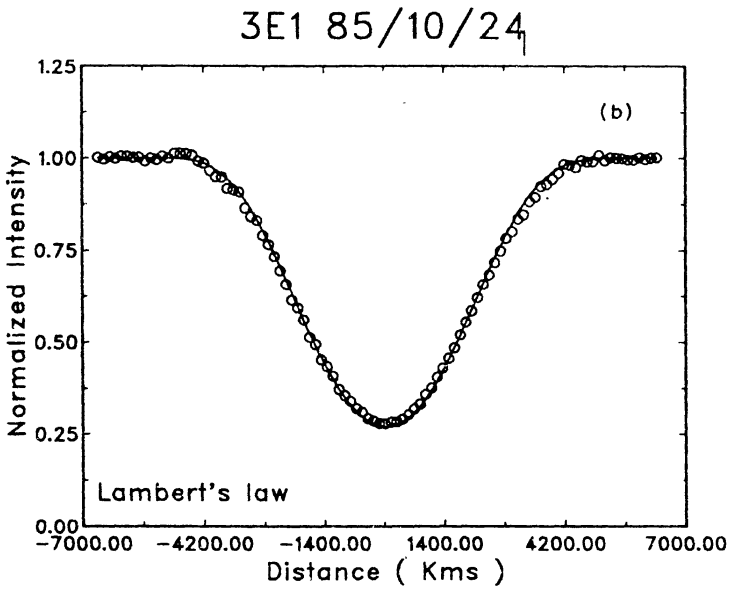

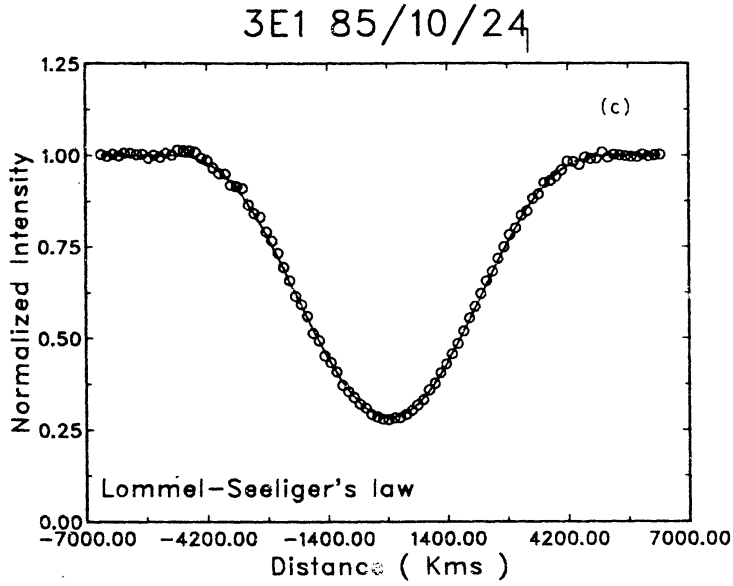

Figure 5. Continued.

Table 4. Fitted impact parameters and δx_{shift}. Assuming $\omega = \mu$ and $p = 1$.

Date (1)	Event (2)	x shift δx_{shift} (kms) (3)	Impact parameter y (kms) (4)	χ^2 (5)	Fig. (6)
85/10/12	1E2	(+65)	691	7.055×10^{-4}	6
85/11/15	3E1	(−45)	336	8.688×10^{-4}	7

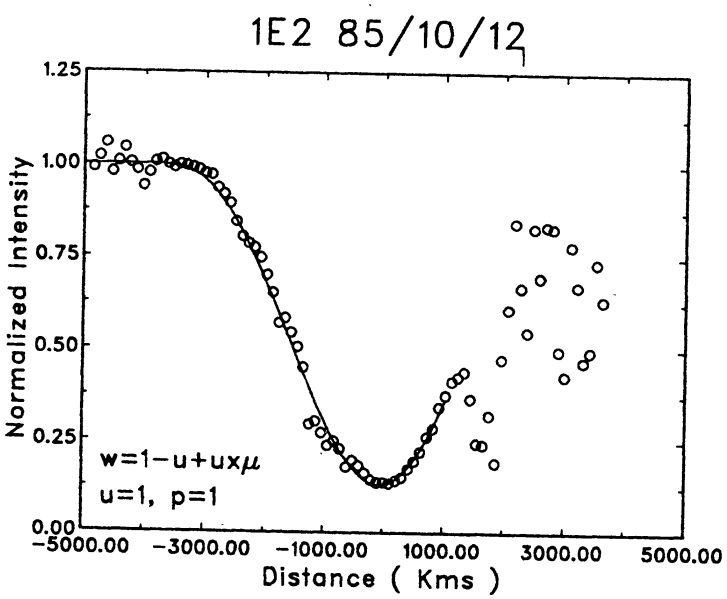

Figure 6. Observed (○) and fitted (continuous line) light curves of 1E2 event on 1985 October 12. The stretch of continuous curve indicates the span of data points used in the fitting process. Results using reflectance law given in Equation 9(c).

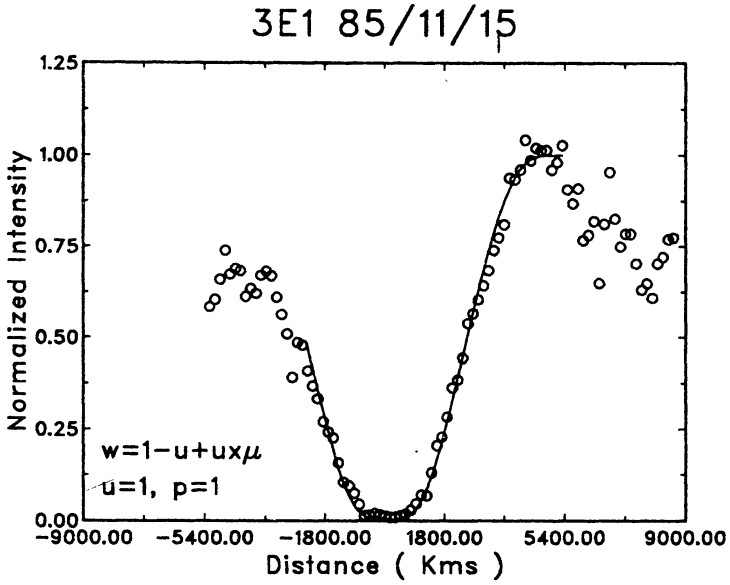

Figure 7. Results of 3E1 event on 1985 November 15. Other details same as that given for Fig. 6.

The finite values of δx_{shift} (given in parentheses) in Tables (2–4) for the uniform disc model and the model using 9(c) arise as a result of fitting the observed slightly asymmetric curve (due to phase effect) with a theoretical symmetric curve.

5. Heliocentric sky plane coordinates

The relative separation between the centres of the two satellites ($\Delta\alpha \cos \delta$, $\Delta\delta$) at close approach as seen from the Sun was calculated from the derived value of the impact

Table 5. Heliocentric ($\Delta\alpha\cos\delta$, $\Delta\delta$) at mid event.

Ut Date (1)	Event (2)	Position Angle (deg) (3)	Impact Parameter (kms) (4)	$\Delta\alpha\cos\delta$ (kms) (5)	$\Delta\delta$ (kms) (6)	Direction of motion (7)
85/09/24	1E2	157.42	328	+126	−303	W−E
85/10/12	1E2	341.80	691	−216	+656	W−E
85/10/24	3E1	342.19	1683	−515	+1602	W−E
85/11/15	3E1	154.33	336	+456	+303	E−W

Table 6. Predicted phase corrections.

UT date (1)	Event (2)	v (kms s^{-1}) $\dot{v}\times10^4$ (kms s^{-2}) (3)	Phase (deg) (4)	Phase corrections δx_{phase} (kms) (5)	Phase corrections δT_{phase} (s) (6)
85/09/24	1E2	+11.926 +5.219	9.3	−78	+6.6
85/10/12	1E2	+15.655 +4.801	10.8	−86	+5.5
85/10/17	3E1	+23.333 −4.689	11.0	−108	+4.6
85/10/24	3E1	+21.403 −5.411	11.3	−105	+4.9
85/11/15	3E1	−1.047 +1.187	11.0	−118	−112.7

parameter y, based on the best fitting model Equation 9(d) using the relations:

$$\Delta\alpha\cos\delta = y\sin(PA)$$
$$\Delta\delta = y\cos(PA) \tag{17}$$

where PA is the predicted position angle of SAT_2 relative to SAT_1 at the time of close approach measured from the north point (Earth's) towards east. The calculated values of PA, $\Delta\alpha\cos\delta$ and $\Delta\delta$ are given in Table 5.

6. Comparison of predicted and observed midtimes

The observed times of light minimum T_{mino} were corrected for the phase effect δT_{phase} (Aksnes, Franklin & Magnusson 1986) to obtain the time of geometric close approach T_{mido} using the relations:

$$\delta T_{\text{phase}} = -\delta x_{\text{phase}}/v$$
$$T_{\text{mido}} = T_{\text{mino}} + \delta T_{\text{phase}}. \tag{18}$$

Table 7. C-O (Mid time).

Ut Date 1985 Event (1)	E-2 Time (s) (2)	E-2 Dist. (kms) (3)	G-5 Time (s) (4)	G-5 Dist. (kms) (5)	AF Time (s) (6)	AF Dist. (kms) (7)	E-3* Time (s) (8)	E-3* Dist. (kms) (9)
24 Sep. 1E2	−15	−181	−5	−62	−44	−527	−12	−145
12 Oct. 1E2	−14	−214	−9	−136	−44	−684	−15	−230
17 Oct. 3E1	+8	+194	+8	+194	−9	−203	+6	+147
24 Oct. 3E1	+12	+259	+7	+152	+2	+45	+11	+238
15 Nov. 3E1	+149	−157	+185	−194	+97	−102	+145	−152

*This work

For each event δx_{phase} was calculated using Equations 13–15 and the scattering law given by 9(d). The sign of δx_{phase} is positive if the geometric centre is to the east of light centre, and v is positive for eastwardly motion of SAT_2 relative to the shadow centre. The phase corrections in distance δx_{phase} and in time δT_{phase} are given in columns 5 and 6 of Table 6. The mid time T_{mido} of the events are given in column 3 of Table 1a. The errors (C–O) in time and distance arising due to error in the theories used in prediction were calculated using the relations

$$\delta T_{\text{er}} = T_{\text{midp}} - T_{\text{mido}}$$
$$\delta x_{\text{er}} = \delta T_{\text{er}} \times v \tag{19}$$

The calculated values of δx_{er} and δT_{er} are given in columns 2–9 of Table 7.

7. Conclusion

The observed mid times of all the events were close to the predicted times except for the slow 3E1 event on 1985 November 15.

Lieske's theory (1980, 1987) is capable of predicting positions of Jovian satellites to an accuracy better than 100 kms. From Tables 2 and 3 it can be seen that differences in the fitted impact parameters, using different scattering laws are also of this order. To extract maximum information from mutual events data, it is therefore essential to use an appropriate model to describe the global reflectance characteristics of the eclipsed or occulted satellites.

Using the data of 3E1 that was obtained under good photometric conditions and using Marquardt's technique for fitting, it appears that Lommel-Seeliger's law leads to best fit over the entire light curve. Although the χ^2 is minimum for solution using Lambert's law for the 1E2 event on 1985 September 24, the fitted curve using Lommel-Seeliger's law matches more closely with observations at apparently cloud free regions;

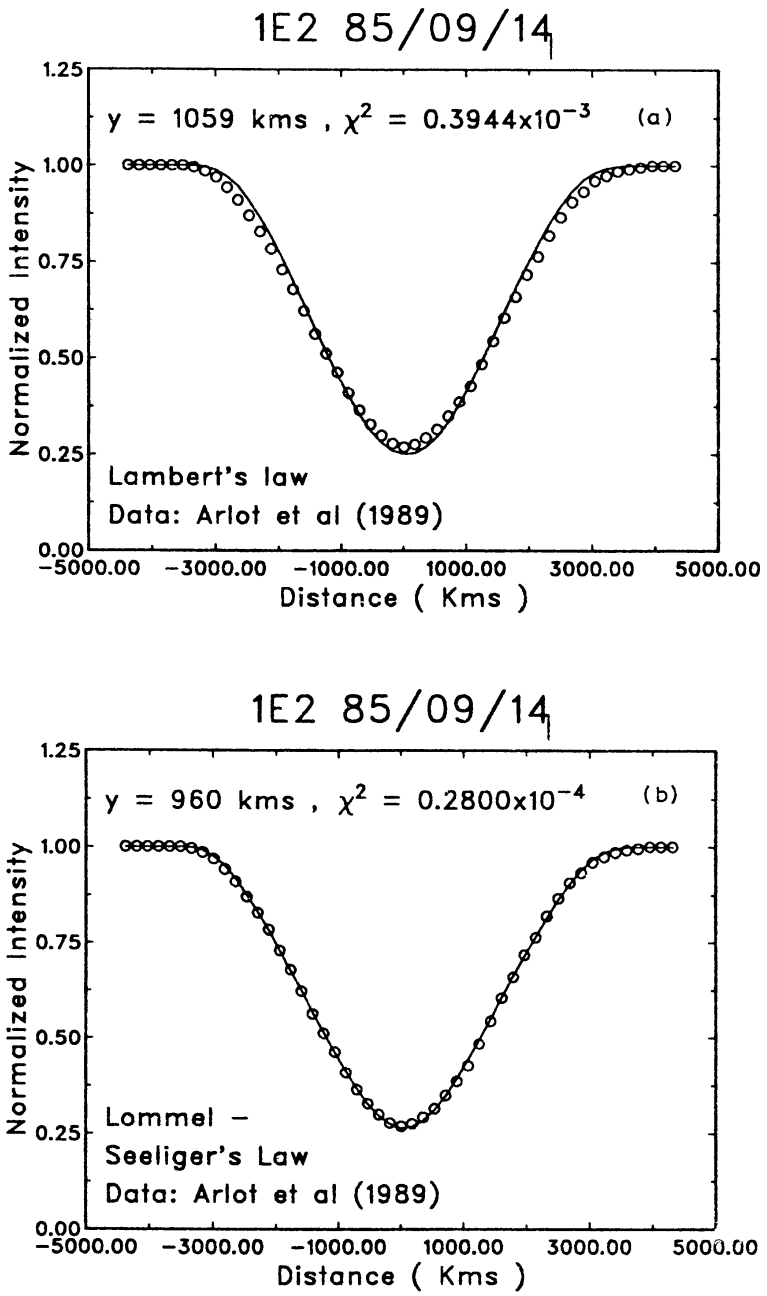

Figure 8. Observed (○) and fitted curves (continuous line) of 1E2 event on 1985 September 14 (Data: Arlot *et al.* 1989); a: using Lambert's law and b: using Lommel-Seeliger's law.

however no definite conclusions can be drawn due to non photometric sky conditions during data acquisition.

Due to poor sky conditions on 1985 October 12 and 1985 November 15, the data were fitted using the scattering law given by 9(c) and no attempt was made to compare results using Lambert's law and Lommel-Seeliger's law.

To confirm the present results, the published high quality light curves of the events 1E2 on 1985 September 14, 3E1 on 1985 September 26 and 2E1 on 1985 October 28 (Arlot *et al.* 1989) were digitized and fitted assuming scattering laws 9(b) and 9(d). The

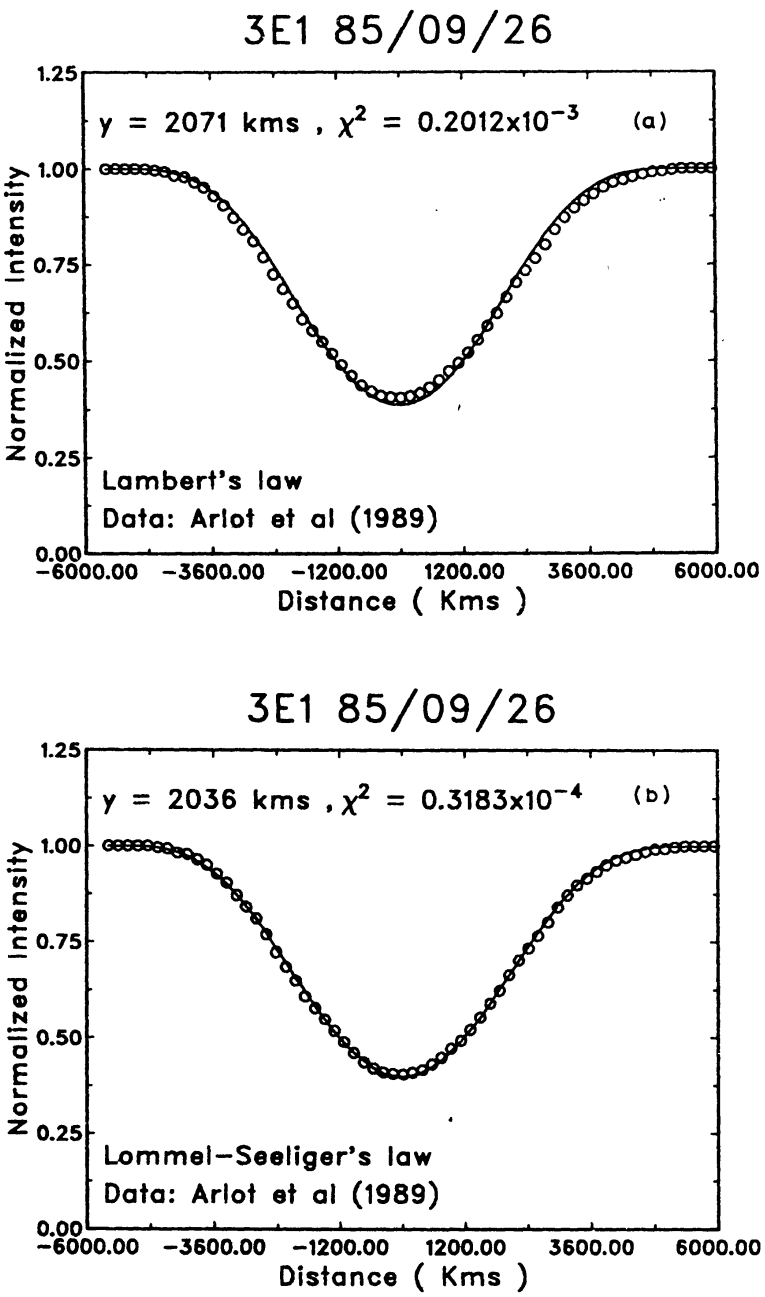

Figure 9. Observed (○) and fitted curves (continuous line) of 3E1 event on 1985 September 26 (Data: Arlot *et al.* 1989); a: using Lambert's law and b: using Lommel-Seeliger's law.

fitted curves are shown in Figs 8(a), (b), 9(a), (b) and 10(a), (b) respectively; again Lommel-Seeliger's law leads to the best fit. The fitted value of δx_{shift} for the 1E2 event on 1985 September 24 matches well with the predicted phase correction but is significantly larger for the 3E1 event on 1985 October 24.

Acknowledgement

The author would like to express gratitude to Prof. J. Lieske for providing the source code for calculating the satellite positions, to Prof. J. C. Bhattacharyya for his guidance

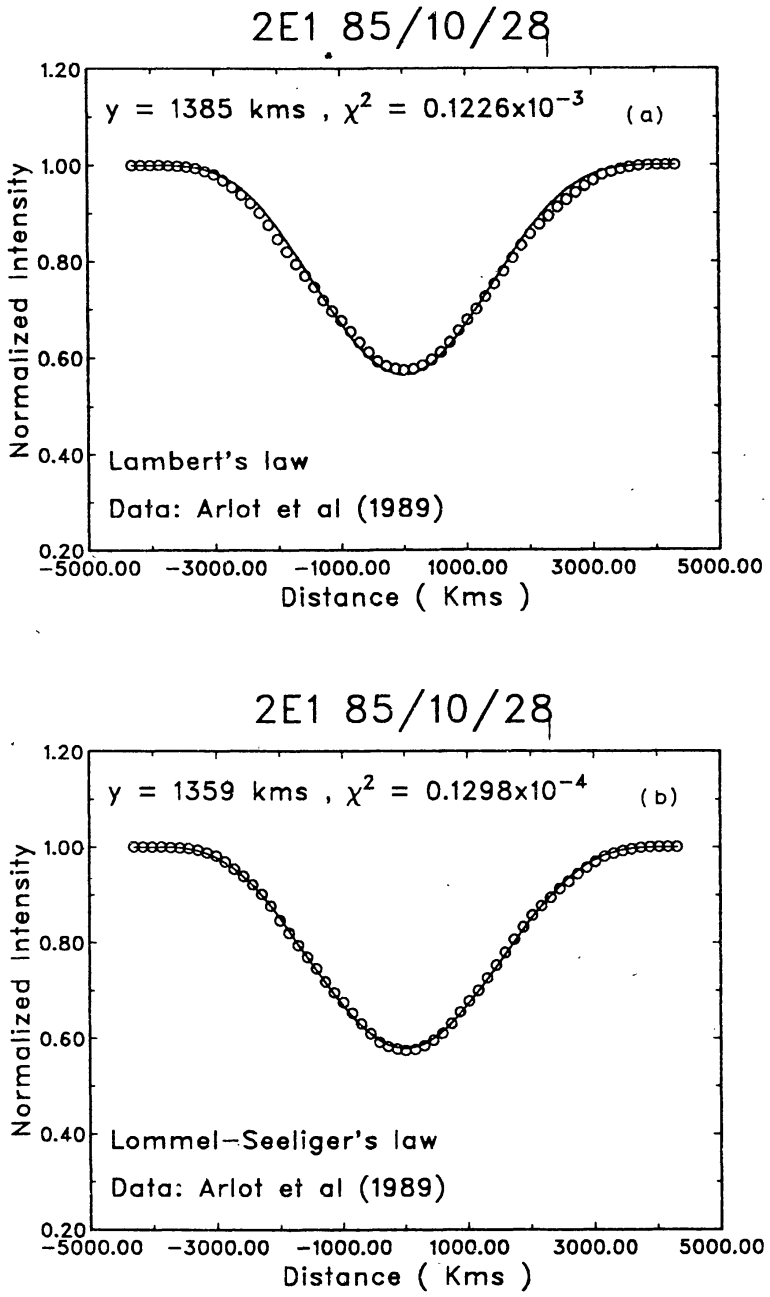

Figure 10. Observed (○) and fitted curves (continuous line) of 2E1 event on 1985 October 28 (Data: Arlot *et al.* 1989); a: using Lambert's law and b: using Lommel-Seeliger's law.

and encouragement in carrying out this project and to Prof. J.-E. Arlot and Prof. D. Morrison for very helpful referees comments.

References

Aksnes, K. A. 1974, *Icarus*, **21,** 100.
Aksnes, K. A., Franklin, F. 1976, *Astr. J.*, **81,** 464.
Aksnes, K. A., Franklin, F. 1984, *Icarus*, **60,** 180.
Aksnes, K. A., Franklin, F., Magnusson, P. 1986, *Astr. J.*, **92,** 1436.

Arlot, J.-E., Camichel, H., Link, F. 1974, *Astr. Astrophys.*, **35,** 115.
Arlot, J.-E. 1982, *Astr. Astrophys.*, **107,** 305
Arlot, J.-E. 1984, *Astr. Astrophys.*, **138,** 113.
Arlot, J.-E., Bouchet, P., Gouiffes, C. H., Schmider, F. X., Thuillot, W. 1989, *Astr. J.*, **98,** 1890.
Bevington, P. R. 1969, *Data Reduction and Error Analysis for the Physical Sciences*, New York, Chapter 11, McGraw-Hill.
Galilean Satellite Observers 1990, *Astr. J.*, (in press).
Lieske, J. H. 1980, *Astr. Astrophys.*, **82,** 340.
Lieske, J. H. 1987, *Astr. Astrophys.*, **176,** 146.
Morrison, D. 1982 in *Satellites of Jupiter*, Ed. D. Morrison, Univ. Arizona press, pp. 3–37.
Surdej, A., Surdej, J. 1978, *Astr. Astrophys.*, **66,** 31.